Superparamagnetic Flexible Substrates Based on Submicron Electrospun Estane® Fibers Containing MnZnFe–Ni Nanoparticles

Pankaj Gupta,[1]* Ramazan Asmatulu,[2] Rick Claus,[2] Garth Wilkes[1]

[1]*Department of Chemical Engineering (0211), Virginia Polytechnic Institute and State University, Blacksburg, Virginia 24061*
[2]*Fiber and Electro Optics Research Center (0356), Virginia Polytechnic Institute and State University, Blacksburg, Virginia 24061*

Received 7 February 2005; accepted 25 July 2005
DOI 10.1002/app.23757
Published online in Wiley InterScience (www.interscience.wiley.com).

ABSTRACT: Flexible, elastomeric, and superparamagnetic substrates were prepared by electrospinning a solution of elastomeric polyurethane containing ferrite nanoparticles (~14 nm) of Mn–Zn–Ni. The flexible mats were characterized in terms of fiber morphology and magnetic properties. Field emission scanning electron microscopy (FESEM) indicated that the diameter of these composite fibers was ~300–500 nm. Furthermore, the back-scattered electron FESEM images indicated agglomeration of the nanoparticles at higher wt % (ca. 17–26 wt %) loading in the electrospun fibers. The induced specific magnetic saturation and the relative permeability were found to increase linearly with increasing wt % loading of the ferrite nanoparticles on the submicron electrospun fibers. A specific magnetic saturation of 1.7–6.3 emu/g at ambient conditions indicated superparamagnetic behavior of these composite electrospun substrates. © 2006 Wiley Periodicals, Inc. J Appl Polym Sci 100: 4935–4942, 2006

Key words: electrospinning; fibers; polyurethane; ferrite nanoparticles; flexible substrates; superparamagnetic behavior

INTRODUCTION

The ability to produce one-dimensional magnetic nanostructures in the form of fibers is very attractive, as these are expected to exhibit interesting magnetic-field-dependent properties. These materials could be used as active components for ultra-high-density storage applications,[1] as well as in the fabrication of sensors.[2,3] Other potential applications include magnetic filters[4] and future generations of electronic, magnetic, and/or photonic devices ranging from information storage, magnetic imaging to static and low frequency magnetic shielding, and magnetic induction.[5–8] One of the commonly used methods to produce one-dimensional nanostructures is based on the electrodeposition of magnetic materials on porous membranes.[9] This technique has been applied to fabricate metallic nanowires that have displayed anisotropic magnetic properties. However, such a technique is limited, when applied to oxide-based magnetic materials (e.g., ferrite), because of the technical difficulties involved in the formation of oxides through the electrochemical deposition process.

Ferrites are widely used in many industrial applications because of their spontaneous magnetization. Therefore, the development of new and cost-effective techniques for fabricating nanostructures based on ferrites is of great commercial and scientific interest. In particular, soft ferrites[10–12] of Mn–Zn, Ni–Zn, and Mg–Mn are well known for their high magnetic permeability.[13] Current research efforts[14] have been focused on synthesizing nanometer-sized (5–20 nm) ferrite particles to minimize energy losses associated with bulk systems. Below a diameter of ~100 nm, particles of mixed[15] ferromagnetic materials (such as ferrites of Mn–Zn–Ni) do not exhibit the cooperative phenomenon of ferromagnetism found in the bulk, as the thermal vibrations are sufficient to reorient the magnetization direction of the magnetic domains.[16] As a result, such nanoparticles display paramagnetic behavior at ambient conditions, thereby imparting a superparamagnetic behavior. When incorporated in submicron (200–500 nm) polymeric fibers, flexible superparamagnetic materials can be produced in a relatively convenient (in comparison to the electrochemical deposition process) and cost-effective fashion. In the present investigation, we report the processing of

Correspondence to: G. Wikes (gwilkes@vt.edu).
*Present address: The Dow Chemical Company, Plastics Materials Science, Freeport, TX 77541.

Contract grant sponsors: The US Army Research Laboratory and the US Army Research Office; contract grant number: DAAD19–02-1–0275.

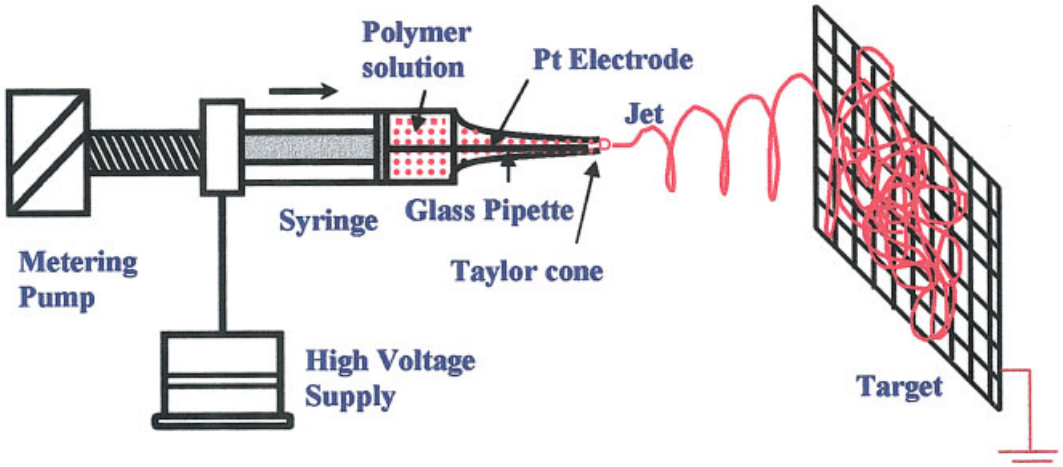

Figure 1 Schematic of the electrospinning apparatus used to electrospin Estane®-MnZnFe–Ni solutions. [Color figure can be viewed in the online issue, which is available at www.interscience.wiley.com.]

such substrates where nanoparticles of a mixed ferrite of Mn–Zn–Ni were incorporated in submicron (200–500 nm) fibers of an elastomeric polymer, Estane® (a polyester based segmented polyurethane), via electrospinning.

Electrospinning is a unique process to produce submicron polymeric fibers in the average diameter range 100 nm–5 μm.[17–20] Fibers produced this way are at least one or two orders of magnitude smaller in diameter than those produced by conventional fiber production methods like melt or solution spinning.[21] In a typical electrospinning process (Fig. 1), described extensively in the literature,[22–26] a jet is ejected from the surface of a charged polymer solution when the applied electric field strength (and consequently, the electrostatic repulsion on the surface of the fluid) overcomes the surface tension. The ejected jet travels rapidly to the collector target located at some distance from the charged polymer solution under the influence of the electric field and becomes collected in the form of a solid polymer filament as the jet dries. During its flight to the target, the jet undergoes a series of electrically driven bending instabilities[27–31] that gives rise to a series of looping and spiraling motions. To minimize the instability caused by the repulsive electrostatic charges, the jet elongates to undergo large amounts of plastic stretching that consequently leads to a significant reduction in its diameter. These extremely small diameter electrospun fibers possess a high aspect ratio that promotes a larger specific surface. As a result, they have potential applications ranging from optical[32,33] and chemo-sensor materials,[34] nanocomposite materials,[35] nanofibers with specific surface chemistry[36] to tissue scaffolds, wound dressings, drug delivery systems,[25,26,37–44] filtration, and protective clothing.[45]

Very recently, magnetic ceramic nanofibers of nickel ferrite were produced by postelectrospinning calcination of PVP/metal alkoxide precursors. The substrates displayed *significant* magnetic hysteresis that could significantly hamper its response in certain high-frequency (MHz) magnetic applications.[13,14] In comparison, electrospinning of a solution containing *well-dispersed* superparamagnetic *nanoparticles* of soft and mixed ferrites leads to the formation of substrates that have very small energy losses because of the absence of the large-scale cooperative magnetic phenomena that is characteristic of bulk ferromagnetic materials.[46] An interesting application of flexible superparamagnetic substrates could be based on their response to high-frequency (MHz) magnetic fields. This becomes relevant where attenuation of the radio signal intensity is required to facilitate better communication in the radio frequency (RF) domain. Such an application is particularly important where radio antennas are embedded in a textile material. In uneven terrain, the signal intensity received by the radio antenna could become very poor, thereby leading to inferior communication.[47] As a result, the need to produce *flexible* superparamagnetic materials that could potentially serve as RF waveguide and antenna materials becomes very relevant. In the present investigation, we report our attempts to process such 'smart' (*flexible, elastomeric, and superparamagnetic*) materials by electrospinning a polymer solution of an elastomeric polymer, Estane®, (a polyester based segmented polyurethane), containing nanoparticles of a mixed ferrite of Mn–Zn–Ni. A similar approach was used by Wang et al.,[16] where superparamagnetic composite polymer/magnetite nanofibers based on water-soluble poly(ethylene oxide) (PEO) and poly(vinyl alcohol) (PVA) were produced. In contrast, Estane® is elastomeric and nonwater-soluble in comparison to PEO and PVA, therefore, it is expected that for certain applications where flexibility might be critical in high-humidity surroundings, superparamagnetic composite fibers of

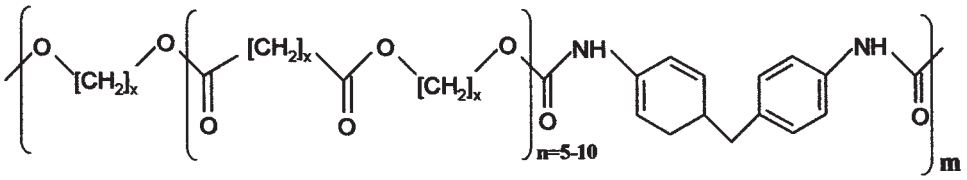

Figure 2 Chemical structure of Estane®.

Estane® will be able display better structural integrity than those based on PEO and PVA. The materials developed by Wang et al.[16] were suggested to be used for reinforcement and nanocomposite applications, whereas the suggested applications of the substrates discussed in the present investigation are different.

EXPERIMENTAL

Materials

Estane® 5750, a polyester-based segmented polyurethane supplied by Noveon Inc., in the form of pellets was used for this study. Molecular weight data for Estane® 5750 could not be obtained, as the information was deemed proprietary, but the generalized chemical structure is depicted in Figure 2. *N,N*-dimethylacetamide (DMAc) was procured from Sigma Aldrich and was used without any further purification. Estane® was dissolved in DMAc at a concentration of 20 wt % by constant stirring for 4 h at 65°C. Superparamagnetic ferrite nanoparticles (~14 nm) based on MnZnFe–Ni, which were dispersed in ethanol at a concentration of 5 and 10 wt %, were procured from NanoSonic Inc. A transmission electron micrograph (TEM) of the nanoparticles is shown in Figure 3. The dark spots that represent the nanoparticles indicate the size to be ~14 nm. The solution of ferrite nanoparticles was mixed with Estane® solution at different ratios to make four solution-blends (Table I). These were subsequently used for electrospinning to make composite electrospun substrates that had various amounts of loading of the nanoparticles on the Estane® fibers. It should be noted that ethanol and DMAc are compatible solvents; as a result, the two solutions were easily mixed to obtain the four-component solutions. However, because of an extremely large ratio of the densities of the polymer and the magnetic nanoparticles (~1 : 7), the heavier nanoparticles in the solution were observed to settle down due to gravity within a period of 48 h, if left undisturbed. Therefore, these solutions were stirred vigorously before electrospinning to achieve sufficient dispersion of the nanoparticles. Each sample was electrospun over a period of ~30 min to obtain a mat thickness of ~170–200 μm.

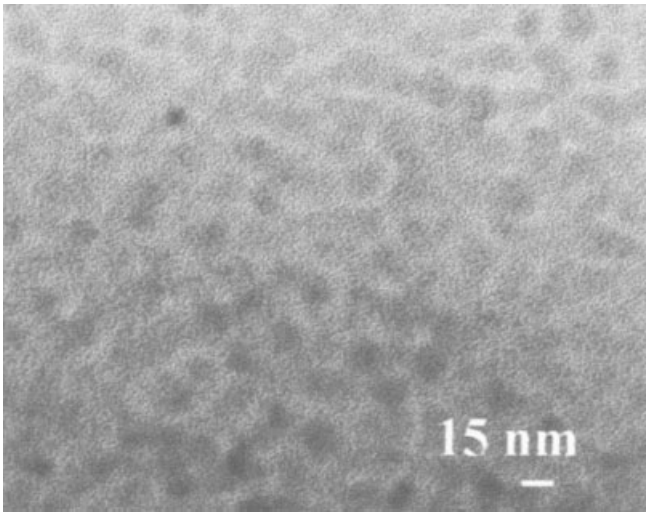

Figure 3 TEM of MnZnFe–Ni nanoparticles.

Electrospinning and characterization

Prior to electrospinning, the viscosities of these solutions were measured with an AR-1000 Rheometer, TA Instruments Inc. The measurement was performed in the continuous ramp mode at room temperature (25°C), using cone and plate geometry. The sample solution was placed between the fixed Peltier plate and a rotating cone (diameter: 4 cm, vertex angle: 2°) attached to the driving motor spindle. The changes in viscosity and shear stress with change in shear rate were measured. A computer interfaced to the equipment recorded the resulting shear stress versus shear rate data. All the solutions investigated in this study displayed shear thinning behavior at high shear rates (viscosity-shear rate curves not shown). The initial slope of the shear stress-shear rate behavior where Newtonian behavior was observed gave the zero shear rate viscosity, η_o. The zero shear viscosities of the four solutions investigated in this study are summarized in Table I. An Oakton® conductivity tester, model TDStestr 20 was utilized to measure the conductivity of the polymer solutions. Prior to its use, the conductivity tester was calibrated by standard solutions procured from VWR Scientific®. The conductivity of the four solutions investigated in the present study is also summarized in Table I.

Electrospinning of these solutions was done on an apparatus depicted in Figure 1. The syringe containing

TABLE I
Characterization of Solutions, Electrospinning Conditions and wt % Loading of Ferrite Nanoparticles on Solid, Dry Composite Fibers

Total solids (polymer and nanoparticles) concentration in solution, (wt %)	Zero shear rate viscosity (Pa s)	Conductivity (μS/cm)	Electrospinning conditions (potential drop, flow rate, and target distance)	Loading of MnZnFe–Ni on solid, dry Estane®-MnZnFe–Ni fibers (wt %)
17.0	3.0 ± 0.02	54	17 kV, 3 mL/h, 15 cm	6
17.7	3.6 ± 0.07	63	18 kV, 3 mL/h, 15 cm	11
16.7	1.9 ± 0.05	97	20 kV, 3 mL/h, 14 cm	18
15.6	1.1 ± 0.18	203	17 kV, 3 mL/h, 14 cm	26

the polymer solution was connected to a Teflon needle (0.7 mm internal diameter). A platinum electrode, placed in the syringe that was immersed in the polymer solution, was connected to a high voltage DC supply at a positive polarity. A syringe-pump connected to the wide-end of the syringe controlled the flow rate emanating out of the Teflon needle tip. Electrospun materials were collected on a grounded steel wire mesh that served as the target kept at ~15 cm from the Teflon tip. The diameter of the steel wire mesh was ~0.5 mm with a mesh count of 20 × 20 (20 steel wires per 1 in. each in the horizontal and vertical axes). All solutions were electrospun at 25°C, 17–20 kV, and 3 mL/h with a 14–15 cm separation distance between the target and Teflon tip (Table I). The fibrous mats were subsequently dried in a vacuum oven for 8 h at 60°C, to minimize any residual solvent.

A Leo® 1550 field emission scanning electron microscope (FESEM) was used to visualize the morphology of the composite electrospun fibers. All the images were taken in the back-scattered mode, as the back-scattered detector is more sensitive to the electron density differences arising due to the presence of different chemical species, viz. ferrite nanoparticles and the polymer. A Cressington® 208HR sputter-coater was used to sputter-coat the electrospun fiber samples with a 10 nm Pt/Au layer to minimize the electron charging effects.

Magnetic properties of composite electrospun substrates were characterized at ambient by using a Lake-Shore 7300 vibrating sample magnetometer (VSM). A sample of ~0.05 g was placed between two coils of an electromagnet that produced a uniform magnetic field gradient. The applied magnetic field induced the magnetic domains to directionally align along the magnetic field. During this induced alignment of the domains, the motion of the ferrite particles produced an electrical signal in a set of stationary pick-up coils that was proportional to the magnetic moment, vibration amplitude, and vibration frequency of the ferrite particles. The magnetic field was ramped from 8000 Gauss to −8000 Gauss and back to 8000 Gauss over a period of 30 min. The magnetic moment of each magnetic sample was measured with a sensitivity of 0.1 emu/g. The specific magnetic saturation values of the composite electrospun substrates were calculated for each electrospun substrate by dividing the saturation magnetization with its mass. Table II lists the specific magnetic saturation in addition to absolute permeability and relative permeability of composite electrospun substrates.

RESULTS AND DISCUSSION

As discussed earlier, four different solutions were made by mixing the Estane® solution (at 20 wt % in DMAc) with the MnZnFe–Ni nanoparticles solutions (at 5 and 10 wt % in ethanol). The total solids concentration of these solutions along with the zero shear viscosity and conductivity of the four solutions are summarized in Table I. The conductivity of the solutions in the present investigation (54–203 μS/cm) was lower than those reported by Wang et al.[16] (329–515 μS/cm) in their investigations. In contrast, the viscos-

TABLE II
Magnetic Saturation, Absolute and Relative Permeability of Estane-MnZnFe–Ni Composite Submicron Fibers

Fiber samples	Magnetic saturation (emu/g)	Absolute permeability[a] (μ) (H/m)	Relative permeability (μ_r)
Estane® w/***6%*** MnZnFe–Ni	1.71	2.26×10^{-6}	1.80
Estane® w/***11%*** MnZnFe–Ni	2.99	3.84×10^{-6}	3.06
Estane® w/***18%*** MnZnFe–Ni	4.38	5.88×10^{-6}	4.68
Estane® w/***26%*** MnZnFe–Ni	6.33	8.23×10^{-6}	6.55
Pure MnZnFe–Ni	25.47	3.45×10^{-5}	27.46

[a] Vacuum permeability 1.257×10^{-6} H/m.

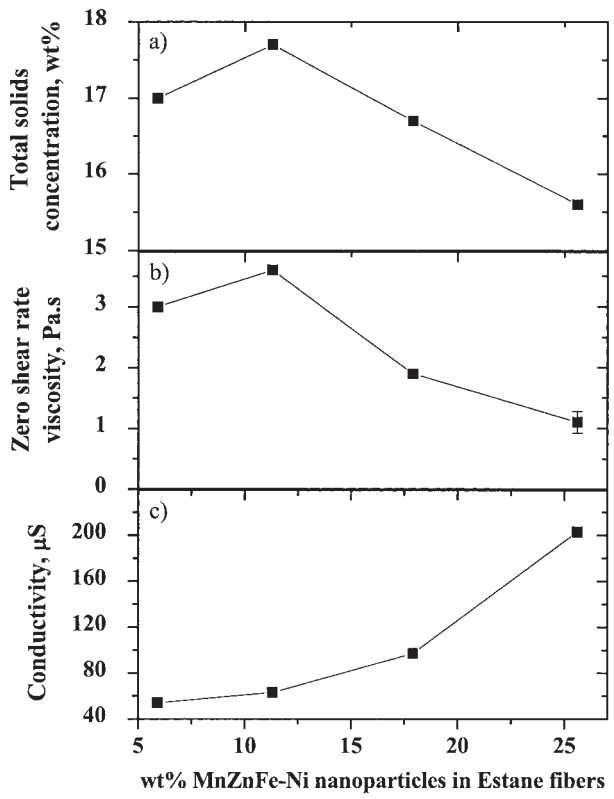

Figure 4 Characterization of solutions. (a) Total solids concentration, (b) Zero shear rate viscosity, and (c) conductivity as a function of wt % of ferrite nanoparticles.

ity of the solutions in the present investigation (1–4 Pa s) was in the same order of magnitude as that measured by Wang et al.[16] (0.8–8 Pa s) in the similar range of concentrations of the solutions investigated. Returning to the data in Table I, it can be seen that the zero shear viscosity follows the same trend as the total concentration solids in ethanol and DMAc when plotted as a function of the wt % loading of nanoparticles on Estane® fibers [Fig. 4(a) and (b)]. Furthermore, the conductivity of the solutions was found to increase with an increase in the loading of the nanoparticles, as was expected (Fig. 4(c)). Electrospinning of these four solutions resulted in four flexile substrates that had different wt % loading (6, 11, 17, and 26 wt %) of MnZnFe–Ni nanoparticles on the Estane® fibers. Interestingly and not surprisingly, all the four flexible composite substrates did not display any electrical conductivity. This result might be useful for certain applications, where magnetic behavior may be desired but without any electrical conductivity, thereby indicating no percolation of the conductive nanoparticle phase.

The backscattered FESEM images of the four substrates, as shown in Figure 5, indicated the electrospun fiber diameter to be ~300–500 nm. This diameter range is slightly higher than that observed by Wang et al.[16] (150–400 nm). This could be explained by the higher conductivities, and consequently higher net charge density of the electrospun jet, of the solutions used in their study. A higher net charge density causes the electrospun jet to experience stronger electrostatic

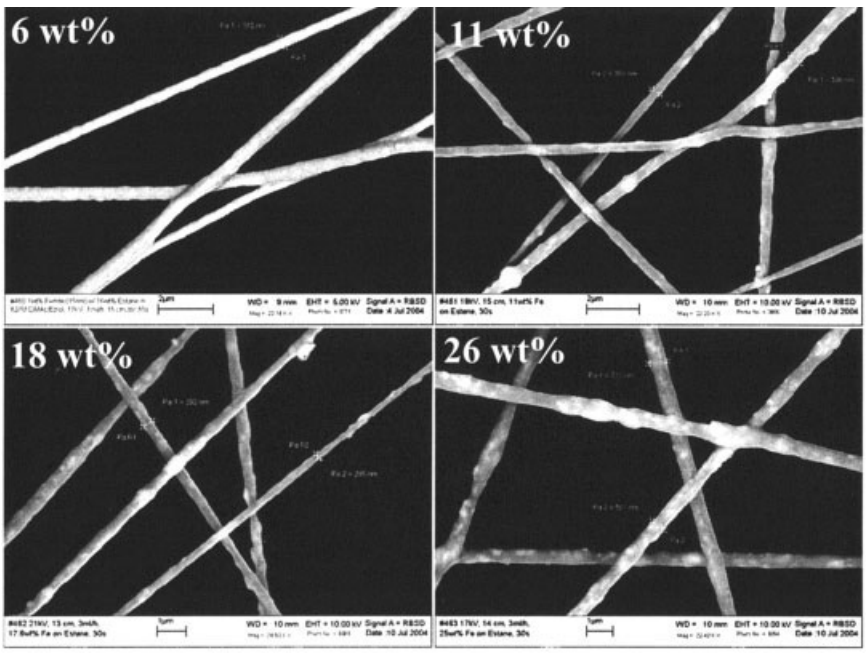

Figure 5 Backscattered SEM images of electrospun Estane®-composite fibers at different concentrations of MnZnFe–Ni nanoparticles. Note the distinctive change in fiber surface contrast at higher loading of nanoparticles. The lighter (high electron density) regions are rich in MnZnFe–Ni nanoparticles.

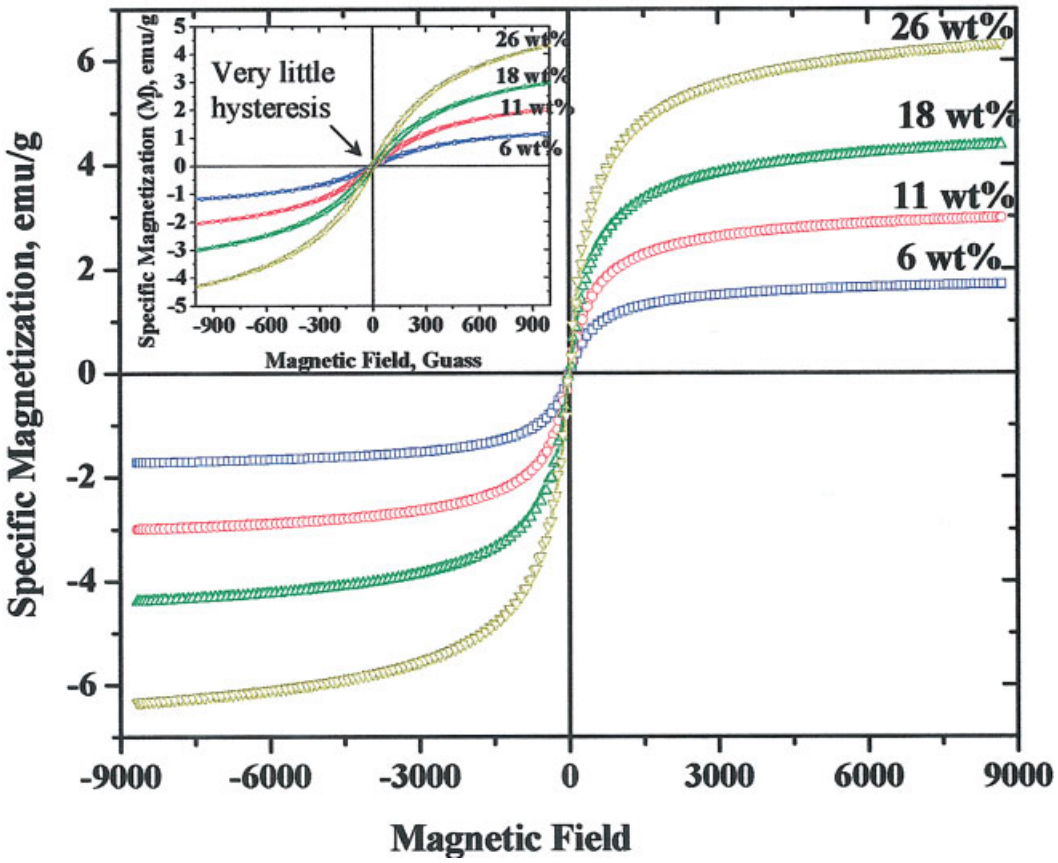

Figure 6 Specific magnetic saturation vs. magnetic field of electrospun Estane®-MnZnFe–Ni composite fibers at different wt % of MnZnFe–Ni nanoparticles. The inset shows the specific magnetization at/and near zero magnetic field region. [Color figure can be viewed in the online issue, which is available at www.interscience.wiley.com.]

forces and as a result higher amounts of plastic stretching.[18]

Although no formal tensile recovery tests were performed on these mats, the composite mats displayed full recovery to small strains (~50%) when stretched between a set of tweezers, thereby indicating the elastomeric nature of these mats. Returning to the data in Figure 5, the high electron density ferrite nanoparticles appeared as whiter spots in these images, which became more apparent at higher wt % loading of the nanoparticles. The increased fiber roughness and larger white spots at higher wt % loading indicated some agglomeration of the nanoparticles in the fibers. However, the agglomeration of the nanoparticles did not affect the overall magnetization behavior of these substrates. This was apparent in Figure 6 where magnetization curves recorded at ambient conditions indicated superparamagnetic behavior of these substrates. The magnitude and direction of the induced specific magnetization varied accordingly with the magnitude and direction of the applied magnetic field. To better observe any magnetic hysteresis, the region close to the origin is enlarged in the inset in Figure 6. It can be clearly seen that these flexible substrates have very little magnetic hysteresis with a small residual magnetization at zero magnetic field. The observed values of the specific magnetic saturation (1–6 emu/g) of the electrospun substrates were very low in comparison to that of bulk materials (~150 emu/g for Fe-Co[46]); however, it is important to note that the bulk materials have relatively larger hysteresis than that observed in ferrite nanoparticles because of the large scale cooperative association of the magnetic domains.[15,46] It is believed that the very little hysteresis in the electrospun substrates investigated in this study, might be critical in governing the magnetic behavior in a high frequency application. As expected, the specific saturation magnetization increased with increasing wt % loading of the nanoparticles as shown in Figure 7(a). A linear correlation between the saturation magnetization and the wt % loading of nanoparticles with a very high regression ($R^2 = 0.999$) was observed. Likewise, the relative permeability, which is the ease with which a magnetic flux can be induced in a material, was also plotted with the wt % loading of the nanoparticles on Estane® fibers. Again, a linear correlation with a high regression coefficient was observed ($R^2 = 0.999$).

These investigations indicate that flexible, elastomeric, and superparamagnetic substrates were suc-

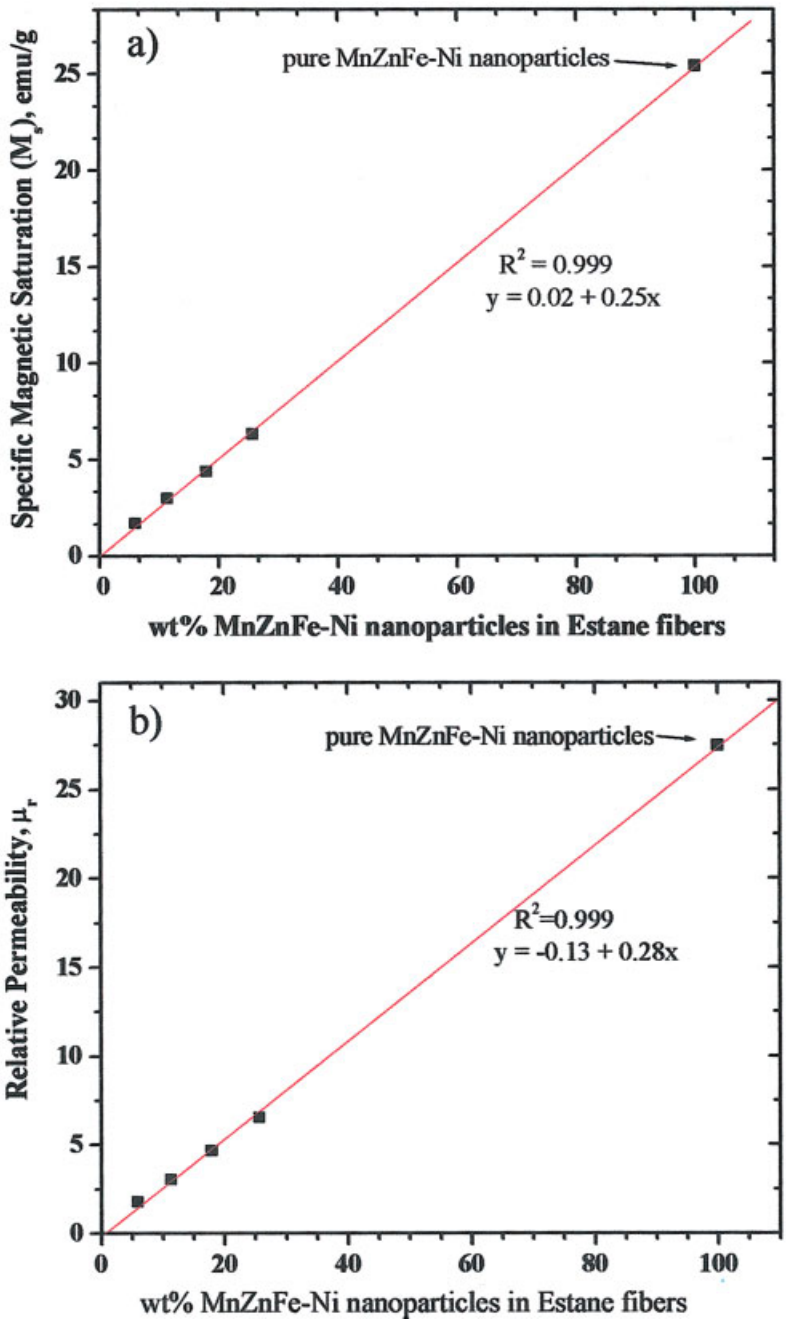

Figure 7 (a) Magnetic saturation (*Ms*) and (b) relative permeability of electrospun Estane®-MnZnFe–Ni composite submicron fibers as a function of wt % of MnZnFe–Ni nanoparticles. [Color figure can be viewed in the online issue, which is available at www.interscience.wiley.com.]

cessfully processed via electrospinning. It would be desirable to conduct further characterization to determine the high frequency (RF, 3–300 MHz) response of these composite mats.

CONCLUSIONS

Flexible, elastomeric, and superparamagnetic substrates were prepared by electrospinning a solution of Estane®, a segmented polyester-based segmented polyurethane, containing ferrite nanoparticles (~14 nm) of mixed Mn–Zn–Ni. The flexible mats were characterized in terms of fiber morphology and magnetic properties. FESEM of the electrospun substrates indicated that the diameter of these composite fibers was ~300–500 nm. Furthermore, the back-scattered electron FESEM images indicated agglomeration of the nanoparticles at higher wt % (ca 17–26 wt %) loading on the electrospun fibers. The induced specific magnetic saturation and the relative permeability were

found to increase with increasing wt % loading of the ferrite nanoparticles on the submicron electrospun fibers. A specific magnetic saturation of 1.7–6.3 emu/g at ambient conditions indicated superparamagnetic behavior of these composite electrospun substrates.

The authors thank Prof. Chip Frazier, Wood Science Department, Virginia Tech, for allowing the use of AR-1000 Rheometer for viscosity measurements.

References

1. Thurn-Albrecht, T.; Schotter, J.; Kastle, G. A.; Emley, N.; Shibauchi, T.; Krusin-Elbaum, L.; Guarini, K.; Black, C. T.; Tuominen, M. T.; Russell, T. P. Science 2000, 290, 2126.
2. Allwood, D. A.; Xiong, G.; Cooke, M. D.; Faulkner, C. C.; Atkinson, D.; Vernier, N.; Cowburn, R. P. Science 2002, 296 2003.
3. Allwood, D. A.; Vernier, N.; Xiong, G.; Cooke, M. D.; Atkinson, D.; Faulkner, C. C.; Cowburn, R. P. Appl Phys Lett 2002, 81, 4005.
4. Markov, E. M.; Pinchuk, L. S.; Goldade, V. A.; Gromyko, Y. V.; Choi, U. S. Trenie i Iznos 1995, 16, 518.
5. Epstein, A. J.; Miller, J. S. Synth Met 1996, 80, 231.
6. Jones, W. E., Jr.; Dong, H.; Nyame, V.; Ochanda, F. Annual Technical Conference—Society of Plastics Engineers 2003, 61 1948.
7. Jones, W. E., Jr. Abstracts of Papers, 226th ACS National Meeting, New York, NY, September 7–11, 2003.
8. Dikeakos, M.; Tung, L. D.; Veres, T.; Stancu, A.; Spinu, L.; Normandin, F. Mater Res Soc Symp Proc 2002, 734, 315.
9. Fert, A.; Piraux, L. J Magn Magn Mater 1999, 200, 338.
10. Snelling, E. C. Soft Ferrites: Properties and Applications; Iliffe Publishers, London, 1969.
11. Snelling, E. C. Proc Brit Ceram Soc 1964, 2, 151.
12. Snelling, E. C. IEEE Spectrum 1972, 9, 42.
13. Thakur, A.; Singh, M. Ceram Int 2003, 29, 505.
14. Morrison, S. A.; Cahill, C. L.; Carpenter, E. E.; Calvin, S.; Harris, V. G. J Appl Phys 2003, 93, 7489.
15. Wang, J.; Zeng, C.; Peng, Z.; Chen, Q. Phys B Condens Matter 2004, 349, 124.
16. Wang, M.; Singh, H.; Hatton, T. A.; Rutledge, G. C. Polymer 2004, 45, 5505.
17. Doshi, J.; Reneker, D. H. J Electrostatics 1995, 35, 151.
18. Fong, H.; Chun, I.; Reneker, D. H. Polymer 1999, 40, 4585.
19. Kim, J.-S.; Reneker, D. H. Polym Eng Sci 1999, 39, 849.
20. Deitzel, J. M.; Kleinmeyer, J. D.; Hirvonen, J. K.; Beck Tan, N. C. Polymer 2001, 42, 8163.
21. Srinivasan, G.; Reneker, D. H. Polym Int 1995, 36, 195.
22. Koombhongse, S. Ph.D. Dissertation, University of Akron, 2001.
23. Koombhongse, S.; Liu, W.; Reneker, D. H. J Polym Sci Part B: Polym Phys 2001, 39, 2598.
24. Schreuder-Gibson, H. International Conference on Textile Coating & Laminating: Preparing for the Future–A New Millenium, 8th, Frankfurt, Germany, November 9–10, 1998. Paper No 17/1.
25. Matthews, J. A.; Wnek, G. E.; Simpson, D. G.; Bowlin, G. L. Biomacromolecules 2002, 3, 232.
26. Matthews, J. A.; Boland, E. D.; Wnek, G. E.; Simpson, D. G.; Bowlin, G. L. J Bioact Compat Polym 2003, 18, 125.
27. Reneker, D. H.; Yarin, A. L.; Fong, H.; Koombhongse, S. J Appl Phys 2000, 87, 4531.
28. Yarin, A. L.; Koombhongse, S.; Reneker, D. H. J Appl Phys 2001, 90, 4836.
29. Yarin, A. L.; Koombhongse, S.; Reneker, D. H. J Appl Phys 2001, 89, 3018.
30. Hohman, M. M.; Shin, M.; Rutledge, G.; Brenner, M. P. Phys Fluid 2001, 13, 2221.
31. Hohman, M. M.; Shin, M.; Rutledge, G.; Brenner, M. P. Phys Fluid 2001, 13, 2201.
32. Wang, X.; Lee, S.-H.; Drew, C.; Senecal, K. J.; Kumar, J.; Samuelson, L. Abstracts of Papers, 222nd ACS National Meeting, Chicago, IL, August 26–30, 2001.
33. Lee, S.-H.; Ku, B.-C.; Wang, X.; Samuelson, L. A.; Kumar, J. Mater Res Soc Symp Proc 2002, 708, 403.
34. Zhang, Y.; Dong, H.; Norris, I. D.; MacDiarmid, A. G.; Jones, W. E., Jr. Abstracts of Papers, 222nd ACS National Meeting, Chicago, IL, August 26–30, 2001.
35. Fong, H.; Liu, W.; Wang, C.-S.; Vaia, R. A. Polymer 2001, 43, 775.
36. Deitzel, J. M.; Kosik, W.; McKnight, S. H.; Tan, N. C. B.; DeSimone, J. M.; Crette, S. Polymer 2002, 43, 1025.
37. Boland, E. D.; Bowlin, G. L.; Simpson, D. G.; Wnek, G. E. Abstracts of Papers, 222nd ACS National Meeting, Chicago, IL, August 26–30, 2001.
38. Boland, E. D.; Matthews, J. A.; Pawlowski, K. J.; Simpson, D. G.; Wnek, G. E.; Bowlin, G. L. Front Biosci 2004, 9, 1422.
39. Boland, E. D.; Simpson, D. G.; Wnek, G. E.; Bowlin, G. L. Polym Preprint 2003, 44, 92.
40. Boland, E. D.; Simpson, D. G.; Wnek, G. E.; Bowlin, G. L. Abstracts of Papers, 226th ACS National Meeting, New York, NY, September 7–11, 2003.
41. Boland, E. D.; Wnek, G. E.; Simpson, D. G.; Pawlowski, K. J.; Bowlin, G. L. J Macromol Sci Pure Appl Chem 2001, A38, 1231.
42. Boland Eugene, D.; Matthews Jamil, A.; Pawlowski Kristin, J.; Simpson David, G.; Wnek Gary, E.; Bowlin Gary, L. Front Biosci 2004, 9, 1422.
43. Kenawy, E.-R.; Bowlin, G. L.; Mansfield, K.; Layman, J.; Sanders, E.; Simpson, D. G.; Wnek, G. E. Polym Preprint 2002, 43, 457.
44. Kenawy, E.-R.; Abdel-Fattah, Y. R. Macromol Biosci 2002, 2, 261.
45. Gibson, P.; Schreuder-Gibson, H.; Pentheny, C. J Coated Fabrics 1998, 28, 63.
46. Tkatch, V. I.; Rassolov, S. G.; Popov, V. V.; Kameneva, V. Y.; Petrenko, O. A. Mater Lett 2004, 58, 2988.
47. Orlicki, J. ACS POLY Workshop on Branched Polymers, Williamsburg, VA, May, 2004.